resources

MDPI

Article

The Use of Phosphogypsum as a Source of Raw Materials for Gypsum-Based Materials

Kseniya Levickaya [1,2], Nataliya Alfimova [2,*], Ivan Nikulin [3,4], Natalia Kozhukhova [1,5] and Aleksander Buryanov [6]

[1] Laboratory of Advanced Materials and Technologies, Belgorod National Research University, 85 Pobedy Str., 308015 Belgorod, Russia; levickayalevickaya@gmail.com (K.L.); kozhuhovanata@yandex.ru (N.K.)
[2] Department of Building Materials Science, Products and Structures, Belgorod State Technological University Named after V.G. Shukhov, 46 Kostyukova Str., 308012 Belgorod, Russia
[3] Engineering Center NRU "BelSU", Belgorod, 2a/712, Koroleva Str., 308033 Belgorod, Russia; ivanikulin@yandex.ru
[4] Fund of Innovative Scientific Technologies, 1, Room 3.3 Perspektivnaya Str. (Novosadovy mkr.), Belgorod Region, Belgorod District, Novosadovy Settlement, 308518 Belgorod, Russia
[5] Department of Material Science and Material Technology, Belgorod State Technological University Named after V.G. Shukhov, 46 Kostyukova Str., 308012 Belgorod, Russia
[6] Department of Building Materials Science, Moscow State University of Civil Engineering (National Research University), 6, Yaroslavskoye Shosse, 129337 Moscow, Russia; rga-service@mail.ru
* Correspondence: alfimovan@mail.ru; Tel.: +7-9205602511

Abstract: Gypsum binders and the products based on them are widely in demand in the construction materials market, which is due to their easy production technology, lower energy consumption, and low environmental impact in relation to Portland cement. Not only natural gypsum (NG), but also phosphogypsum (PG), which is a by-product of the synthesis of orthophosphoric acid from phosphorite rock, can be used as a source of raw materials for the production of gypsum materials. PG is produced annually in large quantities throughout the world. In chemical composition, PG mainly consists of calcium sulfate dihydrate $CaSO_4{\cdot}2H_2O$, so it is a good potential analogue of natural gypsum, which is used as the main component of gypsum building materials. Thus, the useful recycling of PG as a technogenic resource with valuable properties will expand the raw material base for the production of gypsum materials. This approach to handling technogenic resources fits well with the principles of a circular economy. However, like any technogenic resource, PGs from different enterprises normally differ in their deposits of the original phosphate rock and production technologies. Therefore, PG contains a large number of undesirable impurities, the proportion and composition of which vary over a wide range. This feature does not allow for predicting the properties of PG-based materials without a preliminary detailed study of PG. This research was aimed at carrying out a comprehensive study of the characteristics of PGs from three different industrial plants to evaluate their relationship with the properties of gypsum materials based on them. It was found that PGs have significant differences in their structural and morphological characteristics both in relation to each other and in relation to NG. Also, binders based on PG and NG have significant differences in their physical properties. The average density, compressive strength, and flexural strength for the PG binders with equal workability are lower than those of NG binders. At a water/solid ratio (W/S) < 0.7, all PG binders exhibit comparable compressive strength to NG binders. Thus, PG can act as an alternative to natural gypsum in gypsum binders.

Keywords: phosphogypsum; alternative source of gypsum raw materials; by-product; origin characteristics; gypsum binder

check for updates

Citation: Levickaya, K.; Alfimova, N.; Nikulin, I.; Kozhukhova, N.; Buryanov, A. The Use of Phosphogypsum as a Source of Raw Materials for Gypsum-Based Materials. *Resources* **2024**, *13*, 69. https://doi.org/10.3390/resources13050069

Academic Editors: Alberto Bezama, Claudia Arcidiacono, Carlo Ingrao, Jakob Hildebrandt and Annarita Paiano

Received: 20 March 2024
Revised: 7 May 2024
Accepted: 10 May 2024
Published: 14 May 2024

1. Introduction

Gypsum-based materials (plasterboard, blocks, plaster, etc.) are widely in demand in the building materials market due to their easy manufacture, as well as their good physical and mechanical properties (fire resistance, low sound and thermal conductivity, light weight, etc.) [1–3]. It should also be noted that the production of gypsum binders, in comparison with Portland cement, is lower energy consumptive and is also not accompanied by the emissions of harmful impurities and CO_2 into the environment [4,5] (Equation (1)).

$$CaSO_4{\cdot}2H_2O = \beta\text{-}CaSO_4{\cdot}0.5H_2O + 1.5H_2O \tag{1}$$

Normally, natural gypsum (NG) is used for the production of gypsum binders. However, in countries where deposits of NG are limited, gypsum-bearing wastes from various industrial enterprises, such as phosphogypsum, citrogypsum, FGD-gypsum, etc., can be used as an alternative source for gypsum binder production [6–10]. The most large-tonnage of the above-mentioned wastes is phosphogypsum (PG), the annual production of which in the world is ≈300 million tons [8–12].

PG is a primary by-product formed during the production of phosphoric acid and an intermediate product in the production of phosphate fertilizers from phosphate rock (calcium phosphate or apatite) [9–12].

Only 15% of all phosphogypsum produced in the world is recycled; the remaining volume is stored or dumped into water reservoirs, which causes significant damage to the environment [12]. In this connection, the search for ways to use PG as a resource for the production of gypsum binders is a promised trend that will solve the environmental problems in regions where there are accumulations of FG, but will also expand their raw material base for the production of gypsum materials. This concept is in agreement with the principles of the circular economy.

Despite the fact that PG is mainly represented by calcium sulfate dihydrate ($CaSO_4$ $2H_2O$) (Reaction (2)) [13], it also contains impurities of phosphorus, fluorine, organic substances, heavy metals, radioactive substances, etc. [11,14], which can have an ambiguous effect on the quality of gypsum materials. Therefore, PG, as a gypsum-bearing resource, requires additional, more detailed study.

$$Ca_5(PO_4)3F + 5H_2SO_4 + 10H_2O \rightarrow 3H_3PO_4 + 5CaSO_4{\cdot}2H_2O + HF \tag{2}$$

There are a large number of studies where the authors have shown the possibility of obtaining PG-based binders by the heat treatment of phosphogypsum. In particular, according to a number of works studying PG from different countries (China, India, Russian Federation) as a raw material for β-$CaSO_4$ $0.5H_2O$, produced by high-temperature treatment in range of 140–220 °C, it has been established that, despite comparable conditions for the production of PG binders, the compressive strength varies from 4 to 13.8 MPa. There are also significant differences in the setting time [15–20].

This suggests that the quality of PG binders and the gypsum materials based on them is significantly influenced by the origin characteristics of the PG, such as mineralogical and chemical composition, impurities, grain size, etc. In turn, these characteristics depend on the technological parameters of orthophosphoric acid production, as well as the origin of the phosphate rock [9,21]. According to statistical data, 75% of the world's sources of phosphorites are of sedimentary origin and 20–25% are of magmatic origin [9,22,23].

Previous research has mainly focused on the possibility of producing gypsum materials to produce a specific PG component. However, the number of works devoted to the study of the relationship between the characteristics of PGs and the properties of the materials based on them is very limited. At the same time, it is believed that the genetic characteristics of PG (mineral and chemical composition, impurities, grain size, etc.) have a critical impact on the quality of gypsum materials and the efficiency of their production.

This study is aimed at comprehensively investigating the characteristics of PG from three different industrial enterprises to evaluate their relationship to the properties of the gypsum materials based on them.

2. Materials and Methods

The objects of study were the PGs, which were the by-products of the three following Russian enterprises:

1. CJSC PhosAgro AG–PG_{Bal} (Moscow, Russia): Here, the source of raw materials for the production of phosphoric acid is the Khibiny Mine of the alkaline rocks of the Kola Peninsula with sheet- and lens-shaped deposits of complex apatite ores associated with nepheline syenites.

2. Phosphogypsum EuroChem-Belorechenskiye Mineral Fertilizers LLC–PG_{Bel} (Zug, Switzerland): Here, the source of raw materials for the production of phosphoric acid is the apatite concentrate of the Kovdor Mine of ultra-basic alkaline rocks with carbonatites (igneous and metasomatic) of Lower Paleozoic age, as well as phosphorites of the Karatau phosphorite-bearing basin (Republic of Kazakhstan).

3. Phosphogypsum LLC "PG" Phosphorit"–PG_{Kin} (Kingisepp, Russia): Here, the source of raw materials for the production of phosphoric acid is the same as that of PG_{Bel}, but the proportion of raw materials, equipment used, and technology production are different. This may affect the characteristics of the PG and, as a consequence, the gypsum binders based on it.

For this research, the PG sample was used, which was obtained by mixing 20 kg of samples taken from 5 different points of each source.

The reference raw material was NG from the Shedok deposit (Russia).

The chemical and elemental compositions of the studied samples were determined by X-ray fluorescence analysis (XRF), and their mineral composition by X-ray diffraction analysis (XRD). Both methods were realized using an X-ray workstation WorkStation ARL 9900 (Thermo Scientific, Waltham, MA, USA), with co-anode radiation.

Differential thermal analysis (DTA-analysis) was carried out using a thermal analyzer STA 449 F1 JUPITER (Netzsch, Germany).

The study of the microstructure of the PGs and NG particles, as well as the morphology of new formations for synthesized gypsum binders, was carried out with scanning electron (SEM) microscopy using a Mira 3 FesSem scanning electron microscope (Tescan, Czech Republic), operating in high vacuum mode (InBeam) using a Schottky cathode high brightness. The samples were coated with chromium.

The specific surface area (SSA) and the pore size distribution of the PGs and NG particles and the gypsum binders based on them was measured using a multi-functional device PSH-12 (SP) (Khodakov Devices, Moscow, Russia) by Kozeny-Carman gas permeability method. The gas permeability of a powder layer is determined by the duration of air filtration through it at a fixed initial and final vacuum in the working volume of the device.

The Brunauer–Emmett–Teller (BET) and Barrett-Joyner-Halenda (BJH) methods were realized with an automatic device BELSORP miniX (MicrotracBEL Corp., Osaka, Japan). The BET method is a method of mathematical description of physical adsorption, based on the theory of polymolecular (multilayer) adsorption. The BJH method is a method for calculating the pore size distribution in a porous material using adsorption or desorption isotherms. The method is based on the assumption that the pores are cylindrical in shape and that the pore radius is equal to the sum of the Kelvin radius and the thickness of the film adsorbed on the pore wall.

The particle size modulus of PGs was determined using standard methods according to the Russian Standard GOST 8736-2014.

The normal consistency, setting time, compressive, and flexural strength of gypsum binders were determined according to the Russian Standard GOST 23789-2018 and EN 13279-2:2004, NEQ "Gypsum binders. Test methods".

The strength testing of the gypsum samples was carried out using a laboratory press with a load of 10 tons.

The synthesis of the PG binder was carried out using a laboratory oven with electronic temperature control. For the additional monitoring of air temperature and PG temperature in the oven, thermocouples connected to a Mastech MS6514 control and measuring device

(Mastech Digital Inc., Pittsburgh, PA, USA) were used. The temperature of treatment for PG was 175 °C.

3. Results and Discussion

3.1. PGs Characteristics

3.1.1. Chemical and Elemental Composition of PGs

The analysis of the chemical composition (Table 1) and the elemental composition (Table 2) of PG_{Bal}, PG_{Bel}, PG_{Kin}, and NG showed that the studied gypsum bearing components, regardless of origin, are represented by CaO and SO_3 oxides, with the highest content of Ca and S elements, respectively. All PGs contain phosphorus oxide from 0.684 to 1.870%, the amount of which is determined by the chemical composition of the original phosphate rock. The main difference between PGs and NG is the presence, in addition to the main CaO and SO_3 oxides (Table 1) and Ca and S elements, (Table 2), of a large number of additional components, which can subsequently affect the quality characteristics of the binders.

Table 1. Content of oxides in the studied phosphogypsum and natural gypsum and the standard error (StdErr) of the device.

	PG_{Bel}			PG_{Bal}			PG_{Kin}			NG	
Oxide	**%**	**StdErr%**	**Oxide**	**%**	**StdErr%**	**Oxide**	**%**	**StdErr %**	**Oxide**	**%**	**StdErr %**
CaO	47.84	0.250	**SO_3**	48.84	0.250	**CaO**	47.03	0.250	**SO_3**	49.83	0.250
SO_3	47.18	0.250	**CaO**	46.44	0.250	**SO_3**	46.85	0.250	**CaO**	49.62	0.250
P_2O_5	1.87	0.070	**SrO**	2.520	0.080	**P_2O_5**	1.58	0.060	**MgO**	0.14	0.006
SiO_2	1.18	0.050	**P_2O_5**	0.68	0.034	**SiO_2**	1.27	0.060	**SrO**	0.12	0.006
F	1.04	0.180	**CeO_2**	0.36	0.018	**SrO**	1.05	0.050	**Other**	0.30	–
SrO	0.28	0.014	**PuO_2**	0.17	0.010	**F**	0.98	0.170			
MgO	0.15	0.010	**MgO**	0.15	0.008	**Al_2O_3**	0.32	0.016			
Al_2O_3	0.12	0.006	**SiO_2**	0.13	0.009	**CeO_2**	0.22	0.011			
Other	0.35	–	**Fe_2O_3**	0.12	0.006	**MgO**	0.21	0.010			
			Na_2O	0.12	0.018	**Na_2O**	0.10	0.019			
			La_2O_3	0.12	0.009	**Other**	0.40	–			
			Nd_2O_3	0.11	0.006						
			Other	0.23	–						

Table 2. Elemental composition of the studied phosphogypsum and natural gypsum and standard error (StdErr) of the device.

	PG_{Bel}			PG_{Bal}			PG_{Kin}			NG	
Element	**%**	**StdErr%**	**Element**	**%**	**StdErr%**	**Element**	**%**	**StdErr %**	**Element**	**%**	**StdErr %**
Ca	34.21	0.180	**Sx**	19.56	0.100	**CaO**	47.03	0.180	**SO_3**	49.83	0.100
Sx	18.89	0.100	**Ca**	33.21	0.180	**SO_3**	46.85	0.100	**CaO**	49.62	0.180
Px	0.82	0.030	**Sr**	2.130	0.070	**P_2O_5**	1.58	0.027	**MgO**	0.14	0.004
Si	0.55	0.025	**Px**	0.30	0.015	**SiO_2**	1.27	0.026	**SrO**	0.12	0.005
F	1.04	0.180	**Ce**	0.29	0.015	**SrO**	1.05	0.043	**Other**	0.22	–
Sr	0.23	0.012	**Pu**	0.15	0.009	**F**	0.98	0.170			
Mg	0.09	0.006	**Mg**	0.09	0.005	**Al_2O_3**	0.32	0.008			
Al	0.06	0.003	**Si**	0.06	0.004	**CeO_2**	0.22	0.009			
Other	0.29	–	**Fe**	0.09	0.004	**MgO**	0.20	0.006			
			Na	0.09	0.014	**Na_2O**	0.10	0.014			
			La	0.10	0.007	**Other**	0.33	–			
			Nd	0.01	0.005						
			Other	0.17	–						

3.1.2. Mineral Composition of the PGs and NG

The XRD analysis of the studied PGs and NG demonstrated the presence of reflections responsible for the $CaSO_4 \cdot 2H_2O$ phase (d = 7.63, 4.28, 3.80, 3.07, 2.87, 2.69, 2.22, 2.08, 1.90 Å). The intensity of the peaks in the PG patterns varies slightly (Figure 1) among themselves, as well as in comparison with NG. However, it should be noted that PG_{Kin} has the lowest intensity of the main peak (d = 7.63).

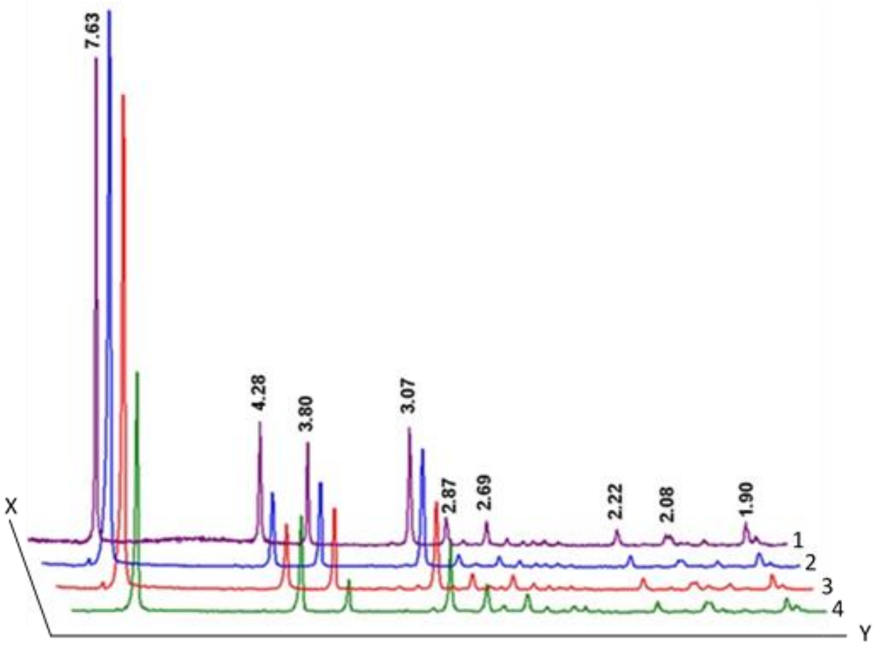

Figure 1. XRD-diagram of PGs and NG. — NG (1); — PG_{Bel} (2); — PG_{Bal} (3); — PG_{Kin} (4).

3.1.3. DTA and TG-Analysis of the PGs and NG

According to DTA-analysis (Figure 2), basic phase transformations, such as the loss of adsorption water (at 100–120 °C); the loss of $0.5H_2O$ (at 220–240 °C); and the inversion of $CaSO_4$ (at 380–420 °C) are characteristic of NG.

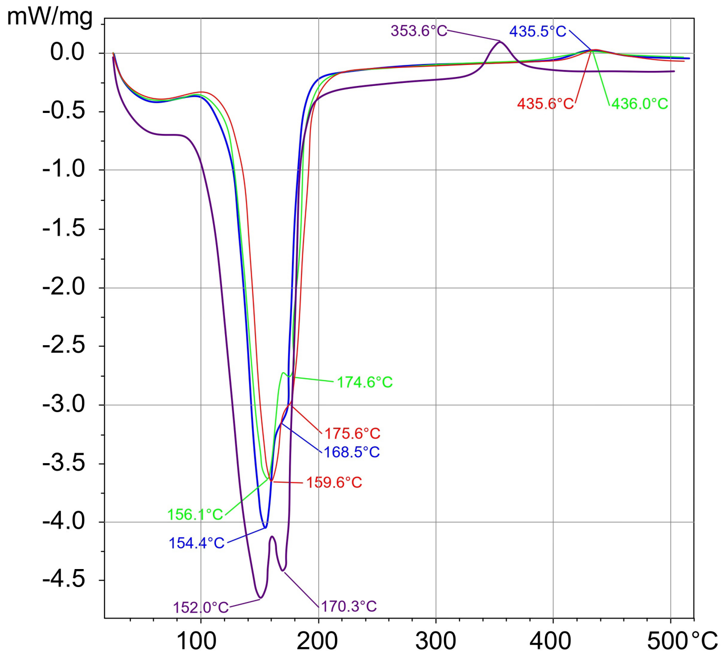

Figure 2. DTA-diagrams of PGs and NG. — NG; — PG_{Bel}; — PG_{Bal}; — PG_{Kin}.

In the case of PGs, the temperature ranges characteristic of the above phase transformations are differ. This is due to the presence of various impurities that can increase or decrease the temperature of phase transformations.

Phase transformations within approximately equal temperature intervals are typical for all PGs. In the DTA diagrams for all PGs and NG, there is a double endothermic effect. The first endothermic peak is associated with the removal of water crystallization during the dehydration of gypsum dihydrate; the second one is associated with the removal of the remaining moisture. However, it should be noted that in the case of PG_{Bel} (Figure 2), the removal of 1.5 of H_2O molecule occurs at a temperature of 154.4 °C, which is 5.2 °C lower than for PG_{Bal} (159.6 °C); PG_{Kin} occupies an intermediate position. For NG, this phase transformation occurs at 152 °C. The formation of soluble anhydrite for PGs occurs in the temperature range of 168.5–175.6 °C, and at 170.3 °C for NG.

Also, the DTA diagrams of PGs have an exothermic peak in the temperature range of 435.5–436 °C, which indicates a restructuring of the crystal lattice with the formation of insoluble anhydrite. In NG, the insoluble anhydrite is formed at lower temperatures: 353.6 °C.

The TG analysis of PGs and NG demonstrated an equal temperature of loss of the adsorbed water. Thus, it can be assumed that replacing NG with PG will not affect the energy consumption of the gypsum binder production process.

3.1.4. Study of the Surface Morphology of PGs and NG Particles

The surface morphology of the PGs particles largely depends on the production technology, the granulometry of the phosphate rock, the concentration of phosphoric acid in the reactor slurry (higher reaction rate, and, as a result, higher ion mobility) and the component ratio.

According to the data in the work presented in [9], there are five morphological types of PG:

(1) The rhombic type is characterized by needle-shaped crystals with a uniform distribution of thin needles and elongated plates with sizes from 10 to 120 μm and crystallite size, normally from 400 to 550 nm;
(2) The aggregate small rhombic type is characterized by small agglomerated needles with a size of 5–30 μm and a crystallite size from 70 to 300 nm;
(3) The cluster type can be characterized as polycrystalline aggregates arranged in a disorderly manner. The crystals tend to form clumps, which are sometimes referred to as “pink sand”;
(4) The aggregate short-needle type is characterized by the presence of small grains, which, normally, have a round, stone-like shape. This type is significantly different from other ones;
(5) The needle type consists of very thin needle-shaped crystals.

The morphology of PGs particles must be taken into account when using it as a raw material for the production of gypsum binders and the materials based on them. For the production of binders and drywall, the most suitable material is PG, which belongs to morphological types 1, 2, and 5. In turn, the types 3 and 4 are mainly used in the cement industry (as an analogue of NG), and in agriculture as well [9].

The analysis of the morphology of the studied PGs showed that PG_{Bel} (Figure 3a) is represented mainly by monoclinic needle-shaped crystals. For PG_{Bal} (Figure 3b), the agglomerates of needles in the sizes of 100–400 μm are observed compared to smaller needle crystals for PG_{Bel}. At the same time, for PG_{Kin} (Figure 3c) there are conglomerates, which are stone-shaped grains with a highly developed surface, in addition to needle-shaped crystals.

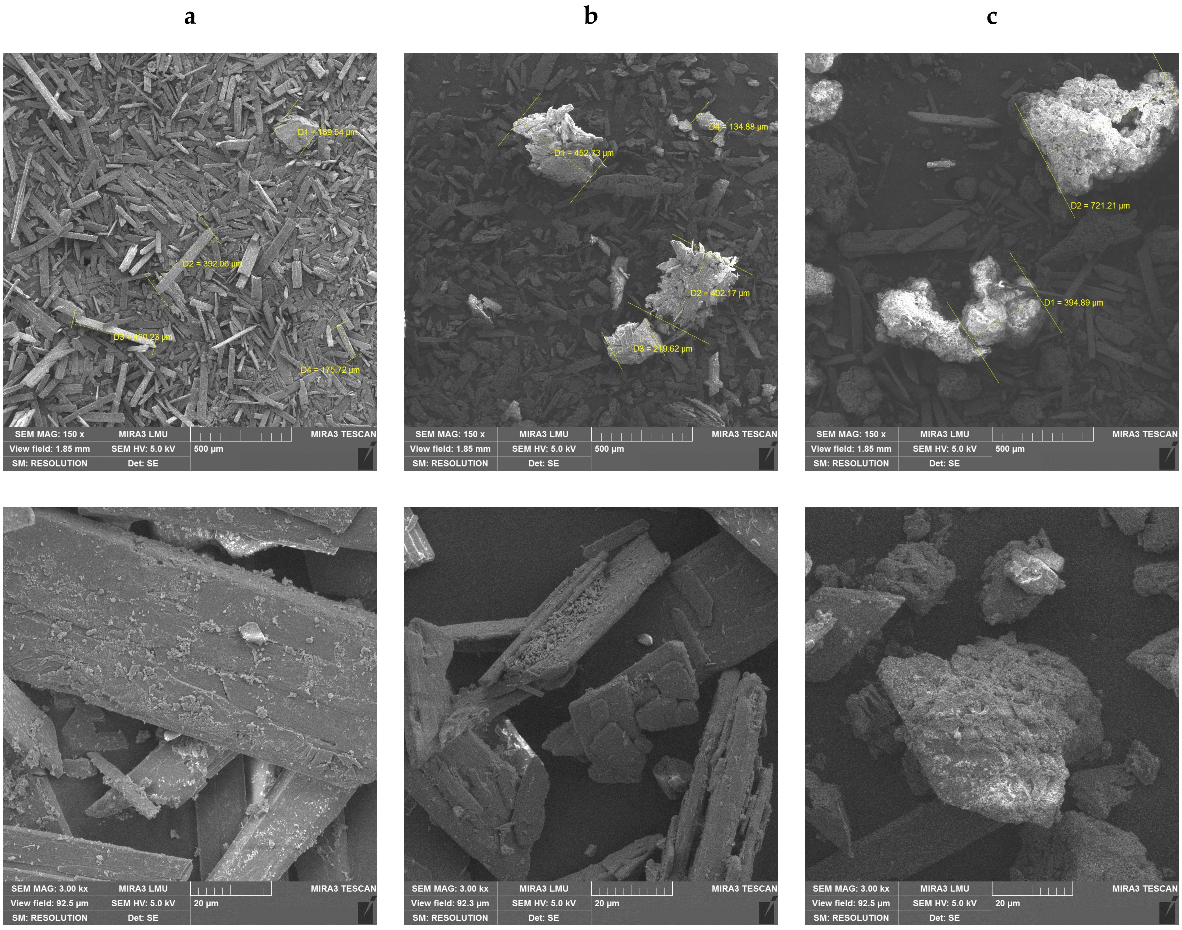

Figure 3. Morphology of the PGs particles. (**a**)—PG_{Bel}; (**b**)—PG_{Bal}; (**c**)—PG_{Kin}.

Thus, morphological analysis showed that PG_{Bel} belongs to the rhombic type; PG_{Bal} is of the small rhombic type; PG_{Kin} is a combination of aggregate and short-needle types.

Despite the identical deposits of phosphate rocks, PG_{Bel} and PG_{Kin} have a significant morphological difference, which is associated with differences in the composition of raw materials, technologies, and equipment used [9].

A comparison of the morphology of NG (Figure 4) showed the presence of a dense, highly developed particle surface (compared to PGs), which is caused by mechanical stress during splitting.

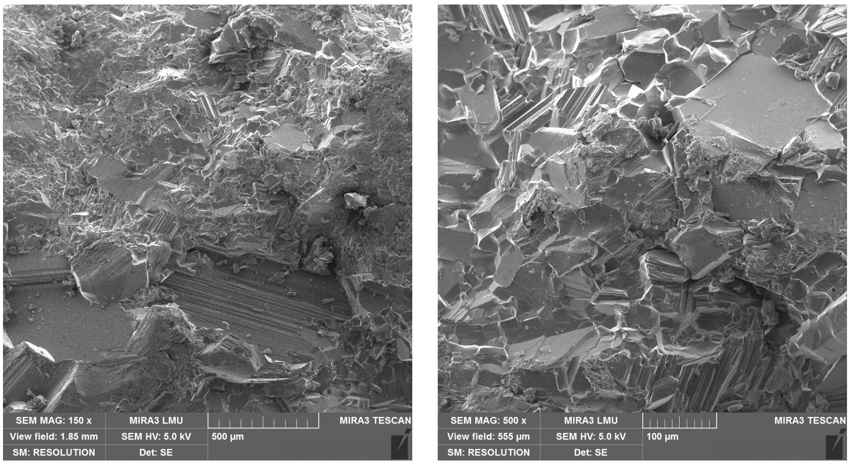

Figure 4. Morphology of the NG.

3.1.5. Study of the Grain Composition and Granulometry of PGs

Visually, the PGs are a bulk material, consisting of small particles and their large associations, formed through the agglomeration of particles during storage under high humidity. Normally, under minor external loads, the destruction of conglomerates occurs.

Figure 5 shows the PG conglomerates selected from the fraction larger than 5 mm. The conglomerates have the following differences in morphology: PG_{Bel} is characterized by a flaky shape (Figure 5a), PG_{Bal} is characterized by a rounded shape with a rounded smooth surface (Figure 5b), and PG_{Kin} has a porous structure and an angular grain shape (Figure 5c).

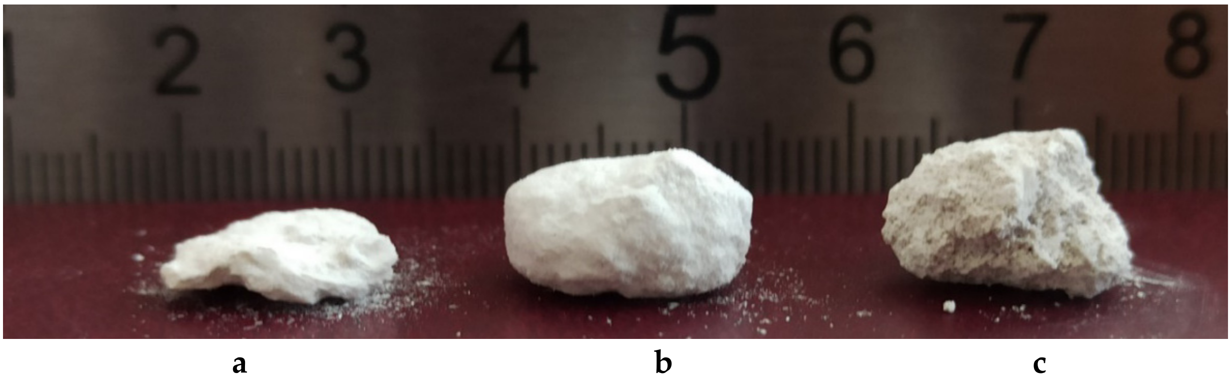

Figure 5. PG conglomerates with a size greater than 10 mm. (**a**)—PG_{Bel}; (**b**)—PG_{Bal}; (**c**)—PG_{Kin}.

The color of PGs varies from white to gray (Figure 6). This depends on the amount and type of impurities in the feedstock, as well as the quality of washing and storage conditions.

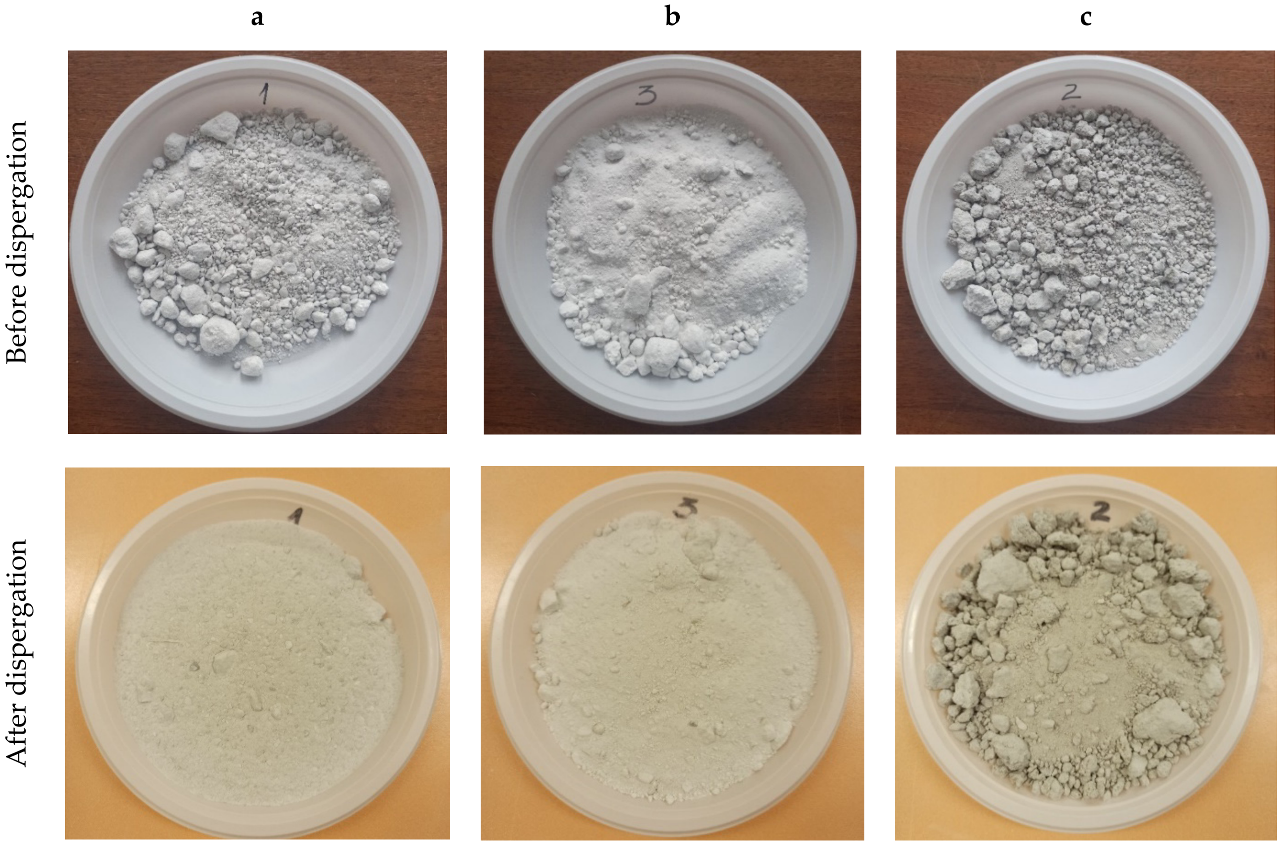

Figure 6. Visual appearance of the PGs: (**a**)—PG_{Bel}; (**b**)—PG_{Bal}; (**c**)—PG_{Kin}.

To determine the fineness modulus, sieving of the PGs was carried out on standard sieves with a mesh size of 0.14; 0.315; 0.63; 1.25; 2.5; 5 mm. Before a sieving test, PGs were dispersed in a plastic container on rollers for 5 min; rubber balls acted as the grinding bodies, which made it possible to reduce the amount of conglomerates without grinding.

It should be noted that in PG_{Kin}, the number of large conglomerates practically did not change, which indicates their high hardness and solidity (Figure 6c).

The grain distribution and fineness modulus of the PGs are given in Table 3. According to the presented data, PG_{Kin} has the largest *f*ineness modulus (2.72), the smallest one is for PG_{Bel} (1.28); the *f*ineness modulusfor PG_{Bal} has an intermediate value (1.89).

Table 3. Grain *distribution* and fineness modulus of the PGs.

PG ID	**Sieve Residue Type**	**Sieve Residue, by wt.% Sieve Mesh Size, mm**							**Fineness Modulus**
		5	**2.5**	**1.25**	**0.63**	**0.315**	**0.16**	**>0.16**	
PG_{Bel}	Partial	8.6	3.9	4.7	7.1	3.9	14.5	57.3	1.28
	Total	8.6	12.5	17.2	24.3	28.2	42.7	100	
PG_{Bal}	Partial	11.2	8.2	6.8	10	7.8	18.9	37.1	1.89
	Total	11.2	19.4	26.2	36.2	44	62.9	100	
PG_{Kin}	Partial	24.6	13.8	8.5	7.8	8.5	14.7	22.0	2.72
	Total	24.6	38.4	46.9	45.7	63.2	77.9	99.9	

SSA measured using the air permeability method for PG_{Bel}, PG_{Bal}, and PG_{Kin} was 203.6 m^2/kg; 183.9 m^2/kg; and 163.5 m^2/kg, respectively.

According to the data from the BET and BJH methods, the maximum SSA is typical for PG_{Bel}, the minimum SSA is for PG_{Bal}, and the SSA value for PG_{Kin} occupies an intermediate position. The analysis of NG showed lower total pore volume values compared to the PGs (Table 4).

Table 4. SSA and the pore size distribution of PGS and NG.

Parameter	$\mathbf{PG_{Bel}}$	$\mathbf{PG_{Bal}}$	$\mathbf{PG_{Kin}}$	**NG**
Air permeability method				
SSA, m^2/kg	203.6	183.9	163.5	–
BET method				
SSA, m^2/kg	18,155	15,773	17,458	–
Total pore volume ($p/p0 = 0.9900$), cm^3/g	0.071	0.067	0.061	0.053
Average pore diameter, nm	15.64	16.98	13.92	14.76
BJH method				
SSA, m^2/kg	18,065	15,717	17172	–
Total pore volume, cm^3/g	0.086	0.084	0.082	0.072
Average pore diameter, nm	19.03	21.40	19.17	19.29

Figure 7 demonstrates the curves of the PGs, representing that the pore volume for a specific diameter are multimodal, and the curve of NG is unimodal. The curve of PG_{Kin} is characterized by four peaks, the two most intense peaks correspond to pore sizes of 3.76 nm (the predominant pore size, see Table 5) and 2.22 nm. The two less intense peaks correspond to particle sizes of 1.93 nm and 2.48 nm. This is most likely due to the fact that PG_{Kin} consists of particles belonging to two different morphological types (Figure 8).

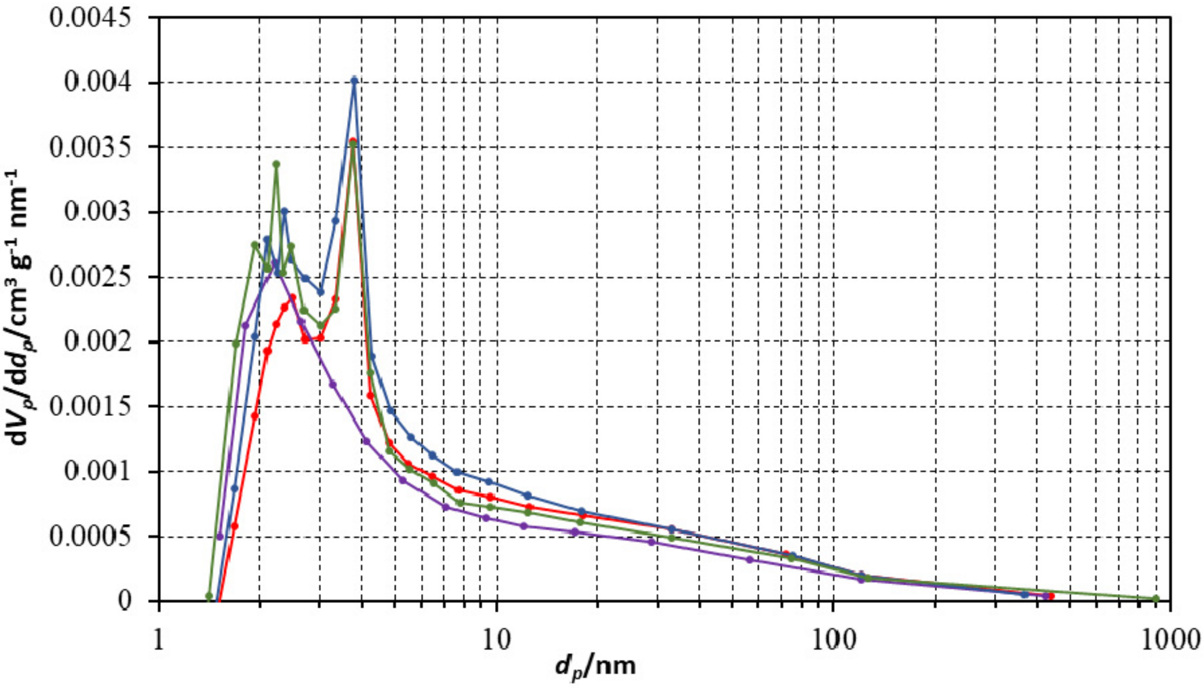

Figure 7. Pore size distribution of PGs and NG. — NaG; — PG_{Bel}; — PG_{Bal}; — PG_{Kin}.

The PG_{Bel} curve is characterized by three peaks: the most intense one corresponds to a pore size of 3.78 nm (Figure 7, Table 5) and two less intensive ones, corresponding to the pore sizes of 2.36 nm and 3.36 nm. PG_{Bal} is characterized by two peaks, corresponding to the pore sizes of 3.76 nm and 2.50 nm. For the curve of NG there is only one peak, corresponding to a pore size of 2.20 nm.

It is assumed that the granulometry of the gypsum-bearing components, as well as the developed surface and porosity of the particles, will influence the amount of mixing water required to ensure the standard consistency of the gypsum binder and, as a result, the strength of the gypsum paste.

At this stage of research, it can be assumed that PG_{Kin}, which is characterized by a smaller pore volume and a larger particle size, is likely to have a lower water requirement to provide a normal gypsum binder consistency compared to PG_{Bel} and PG_{Bal}.

3.2. Study of Binder Characteristics

3.2.1. Study of the Morphology of PG Binders and NG Binder

PG binders were synthesized by the thermal treatment of PGs in a laboratory oven at 175 °C. The NG binder was used as the first reference.

The analysis of the morphology of PG binders showed that thermal treatment does not affect the shape of the particles. However, their surface became more loose and developed due to the detachment of 1.5 of H_2O molecules (Figure 8). It is difficult to judge the effect of thermal treatment on the morphology of particles of the NG binder due to the fact that they are formed by the destruction of the parent rock. At the same time, the surface of the particles of the NG binder has become looser and more developed, just like for PG binders.

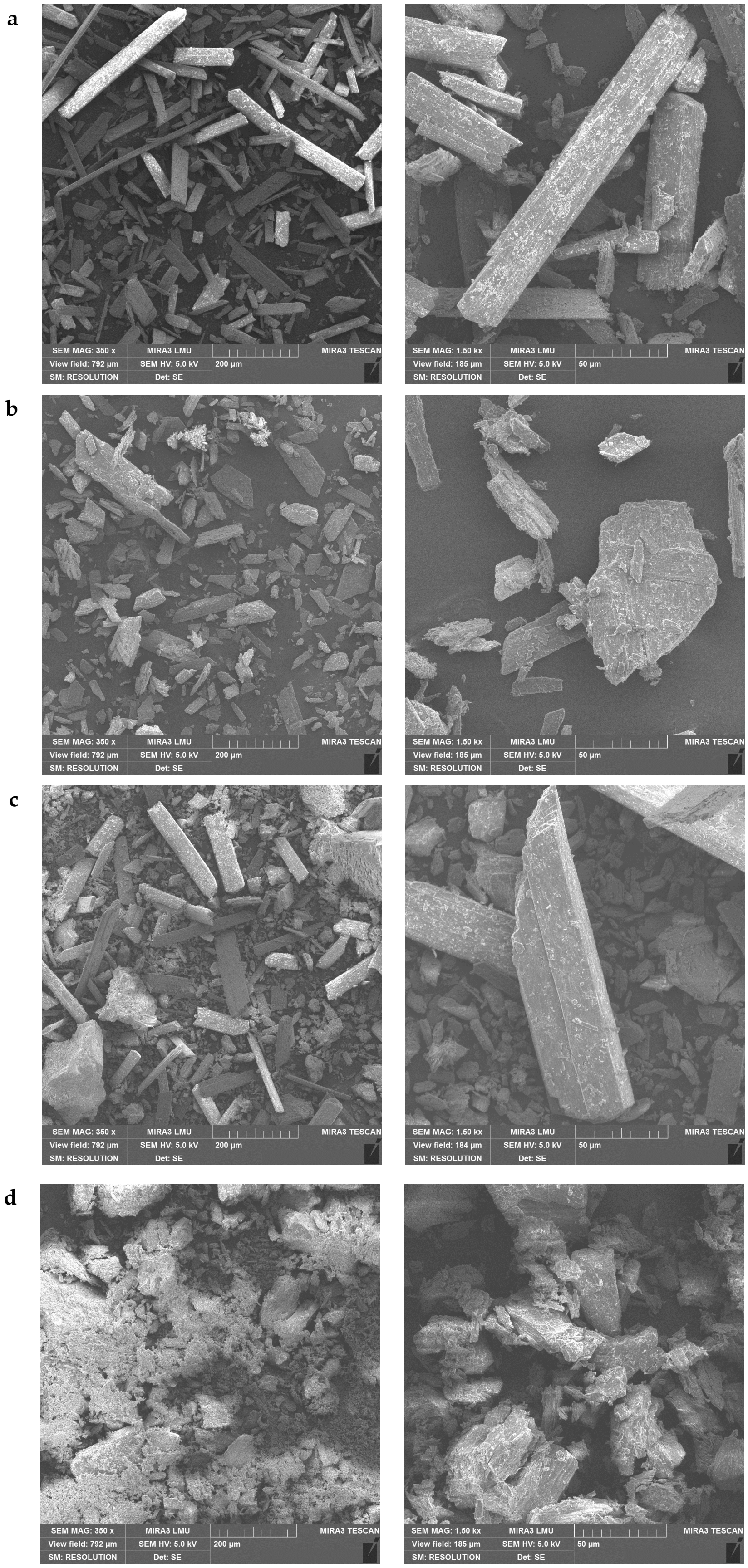

Figure 8. Morphology of the binder based on: (**a**)—PG_{Bel}; (**b**)—PG_{Bal}; (**c**)—PG_{Kin}; (**d**)—NG.

3.2.2. SSA and Pore Size Distribution of the PG Binders and the NG Binder

The SSA, measured by the air permeability method for PG_{Bel}, PG_{Bal}, and PG_{Kin} binders, was 301.0 m^2/kg, 241.8 m^2/kg; and 192.3 m^2/kg, respectively. Thus, the dehydration of PGs during heat treatment contributes to a slight increase in SSA.

The results of the BET and BJH methods demonstrated that the heat treatment of gypsum-bearing components leads to a decrease in SSA and total pore volume, an increase in the average pore diameter, and an increase in the predominant pore size of the binders (Table 5). At the same time, the most noticeable changes in the above parameters were observed for the PG_{Kin} binder.

Table 5. SSA and the pore size distribution of PG binders and the NG binder.

Parameter	Gypsum-Bearing Component			
	PG_{Bel}	PG_{Bal}	PG_{Kin}	NG
Air permeability method				
SSA, m^2/kg	301.0	241.8	192.3	457.0
BET method				
SSA, m^2/kg	5374.9	3633.4	4019.1	4571.8
Total pore volume (p/p0 = 0.9900), cm^3/g	0.040	0.040	0.040	0.038
Average pore diameter, nm	29.66	44.53	40.00	33.11
BJH method				
SSA, m^2/kg	3732.4	2984.5	3506.1	4157.9
Total pore volume, cm^3/g	0.056	0.067	0.068	0.055
Average pore diameter, nm	44.00	90.17	77.93	53.14

Thus, thermal treatment significantly affects the distribution of pores, which is confirmed by a change in the curves reflecting the pore volume distribution (Figure 9), as well as a shift of the peaks towards pores of a larger diameter.

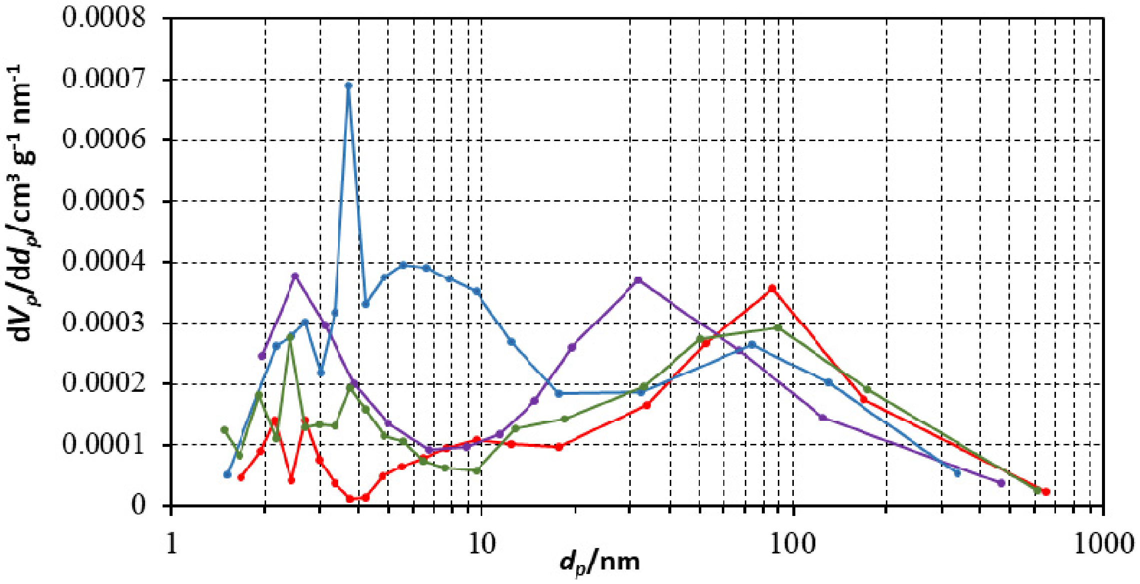

Figure 9. Pore volume distribution for binders, based on: — NG; — PG_{Bel}; — PG_{Bal}; — PG_{Kin}.

3.2.3. Setting Times and Physical Characteristics of the PG Binders and the NG Binder

Setting times, compressive and flexural strength, and average density were determined for the gypsum samples with dimensions of 40 × 40 × 160 mm at the age of 2 h after molding, as well as after the complete drying of the samples. To prepare the gypsum samples, binders with a normal consistency (W/S ratio) were used (Table 6).

Table 6. Physical characteristics of the experimental binders.

Gypsum Component for Binder	W/S ratio	Setting Time, min		Average Density, kg/m^3		Flexural Strength, MPa		Compressive Strength, MPa	
		Initial	Final	after 2 h of Molding	after Complete Drying	after 2 h of Molding	after Complete Drying	after 2 h of Molding	after Complete Drying
PG$_{\mathrm{Bel}}$	0.92	17	22	1461	908	1,.85	2.47	1.72	4.67
PG$_{\mathrm{Bal}}$	0.88	11	19	1457	935	1.90	2.55	2.23	5.29
PG$_{\mathrm{Kin}}$	0.70	15	25	1494	1056	1.91	3.35	3.38	8.14
NG	0.70	18	25	1570	1120	3.11	5.74	4.76	11.96

The analysis of the results in Table 6 showed that to achieve a normal consistency of gypsum binder, the largest amount of water is required for PG$_{\mathrm{Bel}}$ (W/S = 0.92); the least amount of water (W/S = 0.7) is required for the NG binder and the PGB$_{\mathrm{Kin}}$ binder, as well. The higher W/S ratio for the PG$_{\mathrm{Bel}}$ binder results in a longer initial setting time (17 min), compared to the PG$_{\mathrm{Kin}}$ binder (15 min). However, the PG$_{\mathrm{Bal}}$ binder with a high W/S ratio has the shortest initial setting time (11 min). This is most likely due to the different quality of PG washing and, in particular, the higher content of orthophosphoric acid residues in PG$_{\mathrm{Bal}}$, which, according to the literature sources [24], accelerates the initial setting time for the gypsum binder. Interestingly, the studied PG binders are characterized by a faster initial setting time in relation to the NG binder. This is probably also due to the presence of impurities in the PGs that affect the rate of dissolution and precipitation of hydration products.

The average density and strength for the studied PG binders is significantly lower than NG binder both 2 h after molding and after the samples have completely dried. At the same time, the gypsum samples made from the PG$_{\mathrm{Bel}}$ binder have the minimum values of average density and strength, which is due to the high W/S ratio.

When testing these samples at 2 h after molding under a compressive load, moisture was observed on the surface. This suggests that the morphology of the PG$_{\mathrm{Bel}}$ binder and its high SSA initiate its high water demand, which is not used for hydration, but to ensure the normal consistency of gypsum binder. This phenomenon, in turn, negatively affects both the average density and the strength of the gypsum samples.

Despite the equal W/S ratios for the PG$_{\mathrm{Kin}}$ binder and NG binder, the PG$_{\mathrm{Kin}}$ binder has a lower average density and strength, which is likely due to the presence of impurities in the PG, which can affect not only the shape and size of crystals, but also the adhesion between crystals, and increase the total porosity of the gypsum samples which aligns with the data presented in [24].

To study the influence of the W/S ratio on the physical characteristics of the gypsum samples, the cubes with a size of 30 × 30 × 30 mm were molded at the following W/S ratios: 0.5, 0.6, 0.7, 0.8, and 0.9 (Tables 7 and 8).

Table 7. Dependence of the average density of gypsum paste on the W/S ratio and binder type.

Gypsum Component for the Binder	Average Density for Completely Dry Binders at Different W/S Ratios, kg/m^3				
	0.5	0.6	0.7	0.8	0.9
PG$_{\mathrm{Bel}}$	1332	1246	1105	1014	944
PG$_{\mathrm{Bal}}$	1342	1233	1157	1053	927
PG$_{\mathrm{Kin}}$	1321	1202	1095	1062	960
NG	1384	1255	1170	1054	961

Table 8. Dependence of compressive strength of gypsum paste on W/S ratio and binder type.

Gypsum Component for the Binder	Compressive Strength for Completely Dry Binders at Different W/S Ratios, MPa				
	0.5	0.6	0.7	0.8	0.9
PG$_{\mathrm{Bel}}$	16.89	13.96	10.42	8.92	7.57
PG$_{\mathrm{Bal}}$	18.24	15.42	12.21	8.84	7.00
PG$_{\mathrm{Kin}}$	16.94	13.56	10.90	8.22	7.11
NG	16.86	13.96	11.90	9.34	7.50

The analysis of the results (Tables 7 and 8) showed that the average density and compressive strength of completely dry samples gradually decreased with the increasing W/S ratio. With an equal W/S ratio, the values of the average densities do not differ significantly (Table 7), and the values of compressive strength differ significantly depending on the W/S ratio (Table 8).

The compressive strength of the NG samples is higher than the compressive strength of the studied PG binders only at W/S = 0.8. At W/S ratios of 0.5, 0.6, and 0.7, the compressive strength of PG_{Bel} and PG_{Kin} is comparable, but lower than for PG_{Bal}. When the W/S is <0.7, the compressive strength is higher or comparable to the strength of the PG-based samples. At equal W/G ratios, the strength of samples synthesized from PG_{Bel} and PG_{Kin} binders is practically the same. The highest compressive strength at W/G 0.7, 0.6, 0.5 is typical for the PG_{Bal} binder. It was previously established that PG_{Bal} at high W/S ratios (Table 6) has a shorter period of initial setting time than other binders. This indicates an earlier structure formation, which at lower W/S ratios can provide higher strengths than other binders.

It is likely that by using various chemical and mechanical methods to reduce the W/S ratio in PG binders, their physical characteristics may be comparable to or higher than NG binders.

3.2.4. Morphology of New Formations in Gypsum Binders

The SEM analysis of the binders with W/S = 0.6 showed differences in their morphology and the density of new formations. The PG_{Bal} binder (Figure 10b) and NG binder (Figure 10d) are characterized by needle-shaped elongated crystals. New formations in PG_{Bel} and PG_{Kin} binders (Figure 10c) have a prismatic reinforced morphology. The differences in the morphology and size of new formations for the PG binders (Figure 10a–c) can be associated with different contents and types of impurities in PG, which, according to the work presented in [24], have a significant effect on the rate of dissolution and the precipitation of hydration products. In turn, the amount and type of impurities depend on the original phosphate rock, the production technology of orthophosphoric acid, the quality of washing, and the storage conditions of the PG.

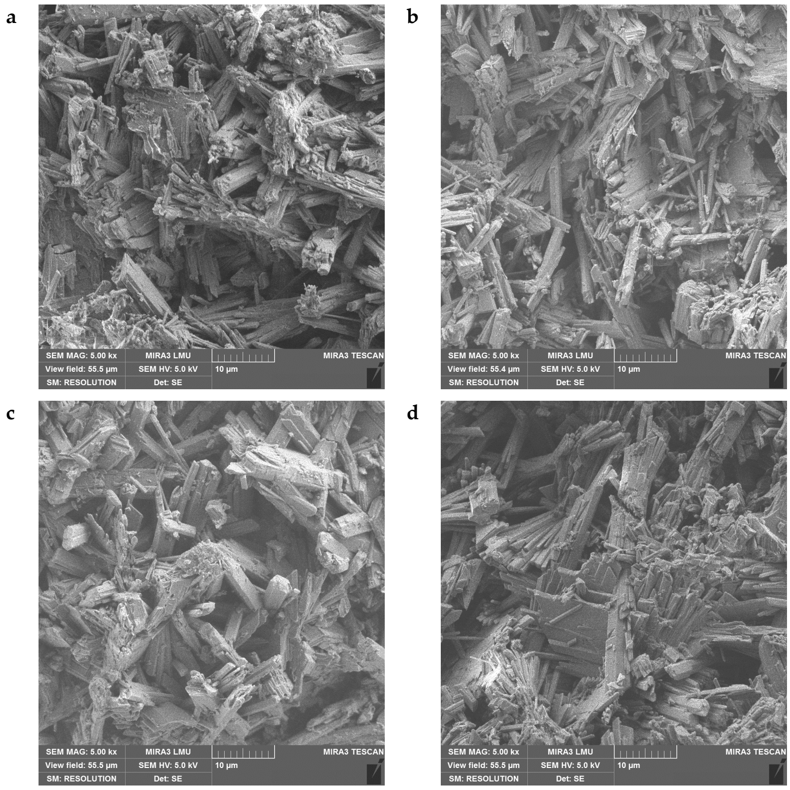

Figure 10. Morphology of the binders based on: (**a**)—PG_{Bel}; (**b**)—PG_{Bal}; (**c**)—PG_{Bal}; (**d**)—NG.

4. Conclusions

A comprehensive study of PG from three different industrial enterprises and its comparison with NG allowed us to obtain the following conclusions:

- all studied PGs can be used as an alternative resource of raw materials to NG when the gypsum binders are synthesized;
- despite the use of the same raw materials for the production of PG_{Bel} and PG_{Kin}, differences in the technological characteristics significantly affect the physical characteristics of PGs and PG materials;
- SSA and pore size distribution for the PG binders are the main factors ensuring a high water demand, and as a result, less satisfactory physical characteristics;
- to increase the efficiency of PGs use as a raw material for the production of PG-based materials, it is necessary to design measures aimed at reducing its water demand, for example, the use of grinding processes and the introduction of superplasticizers.

Author Contributions: Conceptualization, K.L., N.A., N.K., I.N. and A.B.; methodology, K.L., N.A., N.K., I.N. and A.B.; validation, K.L., N.A., N.K., I.N. and A.B.; formal analysis, K.L., N.A., N.K., I.N. and A.B.; investigation, K.L., N.A., N.K., I.N. and A.B.; resources, K.L., N.A. and I.N.; data curation, K.L., N.A., N.K., I.N. and A.B.; Writing—Original draft preparation, K.L., N.A., N.K., I.N. and A.B.; Writing—Review and editing, K.L., N.A., N.K., I.N. and A.B.; supervision, K.L., N.A., N.K., I.N. and A.B.; project administration, K.L. and N.A.; funding acquisition, K.L., N.K. and I.N. All authors have read and agreed to the published version of the manuscript.

Funding: This work was realized under the support of the State Assignment for the creation of new laboratories in 2021, including under the guidance of young promising researchers of the national project "Science and Universities". The research title is "Elaboration and development of scientific and technological foundations for creating an integrated technology for processing gypsum-containing waste from various industrial enterprises and searching of new ways to use processed products", FZWG-2024-0001. Equipment from the High Technology Center at BSTU named after V. G. Shukhov was used.

Institutional Review Board Statement: Not applicable.

Informed Consent Statement: Not applicable.

Data Availability Statement: Data are contained within the article.

Acknowledgments: This work was realized under the administrative support of the world-class scientific and educational center "Innovative Solutions in the Agricultural Sector" (Belgorod).

Conflicts of Interest: The authors declare no conflicts of interest.

References

1. Pedreño-Rojas, M.A.; Fořt, J.; Černý, R.; Rubio-de-Hita, P. Life cycle assessment of natural and recycled gypsum production in the Spanish context. *J. Clean. Prod.* **2020**, *253*, 120056. [CrossRef]
2. Balti, S.; Boudenne, A.; Hamdi, N. Characterization and optimization of eco-friendly gypsum materials using response surface methodology. *J. Build. Eng.* **2023**, *69*, 106219. [CrossRef]
3. Romero-Gómez, M.I.; Costa-Pereira, M.F.; Soares Dias, A.P.; Flores-Colen, I. Influence of high-temperature exposure on the properties of gypsum-plastic waste composites: Thermophysical and microstructural analysis. *J. Build. Eng.* **2023**, *79*, 107862. [CrossRef]
4. Garg, M.; Pundir, A. Energy efficient cement free binder developed from industry waste—A sustainable approach. *Eur. J. Environ. Civ. Eng.* **2017**, *21*, 612–628. [CrossRef]
5. Jain, N.; Maiti, S.; Aakriti, M.J.; Sondhi, D. Development of sustainable water-resistant binder with FGD gypsum & fly ash, and its environmental impact evaluation via carbon footprint and energy consumption analysis. *Sustain. Chem. Pharm.* **2024**, *37*, 101376. [CrossRef]
6. Alfimova, N.; Pirieva, S.; Levickaya, K.; Kozhukhova, N.; Elistratkin, M. The Production of Gypsum Materials with Recycled Citrogypsum Using Semi-Dry Pressing Technology. *Recycling* **2023**, *8*, 34. [CrossRef]
7. Kamarou, M.; Korob, N.; Kwapinski, W.; Romanovski, V. High-quality gypsum binders based on synthetic calcium sulfate dihydrate produced from industrial waste. *J. Ind. Eng. Chem.* **2021**, *100*, 324–332. [CrossRef]
8. Murali, G.; Azab, M. Recent research in utilization of phosphogypsum as building materials: Review. *J. Mater. Res. Technol.* **2023**, *25*, 960–987. [CrossRef]

9. Bilal, E.; Bellefqih, H.; Bourgier, V.; Mazouz, H.; Dumitraş, D.-G.; Bard, F.; Laborde, M.; Caspar, J.P.; Guilhot, B.; Iatan, E.-L.; et al. Phosphogypsum circular economy considerations: A critical review from more than 65 storage sites worldwide. *J. Clean. Prod.* **2023**, *414*, 137561. [CrossRef]
10. Alfimova, N.I.; Pirieva, S.Y.; Elistratkin, M.Y.; Kozhuhova, N.I.; Titenko, A.A. Production methods of binders containing gypsum-bearing wastes: A review. *Bull. BSTU Named V.G. Shukhov* **2020**, *11*, 8–23. [CrossRef]
11. Qin, X.; Cao, Y.; Guan, H.; Hu, Q.; Liu, Z.; Xu, J.; Hu, B.; Zhang, Z.; Luo, R. Resource utilization and development of phosphogypsum-based materials in civil engineering. *J. Clean. Prod.* **2023**, *387*, 135858. [CrossRef]
12. Rashad, A.M. Phosphogypsum as a construction material. *J. Clean. Prod.* **2017**, *166*, 732–743. [CrossRef]
13. Geraldo, R.H.; Costa, A.R.D.; Kanai, J.; Silva, J.S.; Souza, J.D.; Andrade, H.M.C.; Gonçalves, J.P.; Fontanini, P.S.P.; Camarini, G. Calcination parameters on phosphogypsum waste recycling. *Constr. Build. Mater.* **2020**, *256*, 119406. [CrossRef]
14. Seraya, N.; Litvinov, V.; Daumova, G.; Zhusipov, N.; Idrisheva, Z.; Aubakirova, R. Production Waste Management: Qualitative and Quantitative Characteristics and the Calculation of the Hazard Class of Phosphogypsum. *Processes* **2023**, *11*, 3033. [CrossRef]
15. Zhang, L.; Mo, K.H.; Tan, T.H.; Hung, C.-C.; Yap, S.P.; Ling, T.-C. Influence of calcination and GGBS addition in preparing β-hemihydrate synthetic gypsum from phosphogypsum. *Case Stud. Constr. Mater.* **2023**, *19*, e02259. [CrossRef]
16. Cao, W.; Yi, W.; Peng, J.; Li, J.; Yin, S. Recycling of phosphogypsum to prepare gypsum plaster: Effect of calcination temperature. *J. Build. Eng.* **2022**, *45*, 103511. [CrossRef]
17. Jin, Z.; Ma, B.; Su, Y.; Qi, H.; Lu, W.; Zhang, T. Preparation of eco-friendly lightweight gypsum: Use of beta-hemihydrate phosphogypsum and expanded polystyrene particles. *Constr. Build. Mater.* **2021**, *297*, 123837. [CrossRef]
18. Ma, B.; Jin, Z.; Su, Y.; Lu, W.; Qi, H.; Hu, P. Utilization of hemihydrate phosphogypsum for the preparation of porous sound absorbing material. *Constr. Build. Mater.* **2020**, *234*, 117346. [CrossRef]
19. Garg, M.; Pundir, A.; Singh, R. Modifications in water resistance and engineering properties of β-calcium sulphate hemihydrate plaster-superplasticizer blends. *Mater. Struct.* **2016**, *49*, 3253–3263. [CrossRef]
20. Iglenkova, M.G.; Rodina, A.A.; Reshetov, V.A.; Romadenkina, S.B.; Kruzhalov, A.V. Dependences of Durability Phosphogypsum Knitting Materials from the Temperature of Heat Treatment and Particle Size Distribution. *Proc. Saratov Univ. New Epis. Ser. Chem. Biol. Ecol.* **2011**, *11*, 60–63.
21. Loureiro, F.E.L.; de M. Monte, M.B.; Nascimento, M. Agrominerais—Fosfato. In *Rochas & Minerais Industriais usos e Especificações. 2a*; da Luz, A.B., Lins, F.A.F., Eds.; CETEM—Centro de Tecnologia Mineral: Rio de Janeiro, Brazil, 2008; 974p.
22. Pufahl, P.K.; Groat, L.A. Sedimentary and igneous phosphate deposits: Formation and exploration: An invited paper. *Econ. Geol.* **2017**, *112*, 483–516. [CrossRef]
23. Ptáček, P. *Apatites and Their Synthetic Analogues—Synthesis. Structure. Properties and Applications*; InTech: London, UK, 2016. [CrossRef]
24. Jia, R.; Wang, Q.; Luo, T. Reuse of phosphogypsum as hemihydrate gypsum: The negative effect and content control of H_3PO_4. *Resour. Conserv. Recycl.* **2021**, *174*, 105830. [CrossRef]